GEOPHYSICAL RESEARCH LETTERS, VOL. 31, L18111, doi:10.1029/2004GL020384, 2004

Satellite observations of spatial and interannual variability of lightning and radar reflectivity

S. L. Durden, J. P. Meagher, and Z. S. Haddad
Jet Propulsion Laboratory, California Institute of Technology, Pasadena, California, USA

Received 28 April 2004; revised 17 June 2004; accepted 26 August 2004; published 25 September 2004.

[1] The authors use satellite data to examine the relationship between lightning and upper-level radar reflectivity. They find correlations between average flash rates and upper-level reflectivities over both land and ocean, although both flash rates and reflectivities are much lower over ocean than land. Analysis of the data using Empirical Orthogonal Functions (EOFs) shows similar EOFs for averaged lightning and reflectivity. In contrast, the EOFs of the anomalies of lightning and reflectivity have different spatial patterns; however, both have principal component time series that are correlated with the Southern Oscillation Index and, hence, El Niño. Differences in behavior of the lightning and reflectivity anomaly EOFs and principal components suggest that El Niño plays a smaller role in lightning anomaly than precipitation anomaly. *INDEX TERMS:* 3309 Meteorology and Atmospheric Dynamics: Climatology (1620); 3324 Meteorology and Atmospheric Dynamics: Lightning; 3354 Meteorology and Atmospheric Dynamics: Precipitation (1854); 3360 Meteorology and Atmospheric Dynamics: Remote sensing. **Citation:** Durden, S. L., J. P. Meagher, and Z. S. Haddad (2004), Satellite observations of spatial and interannual variability of lightning and radar reflectivity, *Geophys. Res. Lett.*, *31*, L18111, doi:10.1029/2004GL020384.

1. Introduction

[2] The production of lightning by thunderstorms depends on the existence of one or more charging mechanisms. Generally, non-inductive charging mechanisms require collisions between small ice crystals and graupel that is growing by riming [*MacGorman and Rust*, 1998]. Graupel and super-cooled water are expected to provide relatively large radar reflectivities at upper levels in thunderstorms (i.e., above the freezing level). Indeed, *Zipser and Lutz* [1994] show that the presence of large upper-level reflectivities is a good indicator of lightning. The availability of satellite observations of both lightning and reflectivity in thunderstorms allows examination of the relation between lightning and hydrometeors above the freezing level on a global basis. *Petersen and Rutledge* [2001] and *Toracinta et al.* [2002] have carried out such investigations using observations by the Tropical Rainfall Measuring Mission (TRMM) Precipitation Radar and Lightning Imaging Sensor. These investigations have confirmed the relation of lightning to presence of large particles above the freezing level and have discussed the variation of these parameters from region to region. A key spatial dependence noted in these and other works [e.g., *Christian et al.*, 2003] is the much more frequent occurrence of lightning over land than ocean.

[3] One approach for study of spatial and temporal variability is empirical orthogonal functions (EOFs). *Martin et al.* [2000] present the first and perhaps only use of EOFs to describe lightning behavior; they present EOFs for lightning estimates by *Price et al.* [1997] and for measurements of ozone production. They noted that the second ozone EOF behaves like the lightning EOF computed from the *Price et al.* [1997] study. We build on these previous studies by using somewhat longer records of TRMM satellite data to examine correlations between lightning flash rate, upper-level reflectivity, and surface rainfall. We then apply EOF analysis to the flash rate and reflectivity and, more interestingly, to their anomalies.

2. Data and Methodology

[4] The data used here are derived from Level 3 averaged and gridded products. Surface rainfall is available in the TRMM 3B31 product. The upper-level reflectivity is taken from the TRMM 3A25 product. Ideally, this reflectivity would be an average over a layer with temperature range corresponding to the mixed phase region. Since the 3A25 reflectivity is only available at altitudes of 2, 4, 6, 10, and 15 km, we use the reflectivity at 6 km. Lightning information is taken from the Low-Resolution Time Series product of the TRMM Lightning Imaging Sensor (LIS) and its predecessor, the Optical Transient Detector (OTD) [*Christian et al.*, 2003]. The lightning flash rate, 6-km altitude reflectivity, and surface rain rate were sub-sampled and averaged to yield three datasets aligned in time and space, consisting of quarterly averages sampled at 5-degree grid spacing. Thus, spatio-temporal averages of each quantity can be compared at a given point in space and time. EOFs are computed by forming a one-dimensional vector from the two-dimensional spatial data for each quarter, computing the covariance matrix using all quarters, and calculating eigenvectors, which are the EOFs. Principal components are found by projecting the data at each point in time along the EOFs, yielding a time series for each EOF. The TRMM satellite was boosted from 350 km altitude to 400 km altitude in August 2001. To eliminate possible effects of the boost on radar calibration, only pre-boost data were used for the reflectivity EOF analyses. Dates used in the various analyses are provided in the corresponding figure captions.

3. Results

[5] Figure 1 (top) shows the reflectivity in dBZ versus the flash rate on a logarithmic scale. Each point on the plot

Copyright 2004 by the American Geophysical Union.
0094-8276/04/2004GL020384$05.00

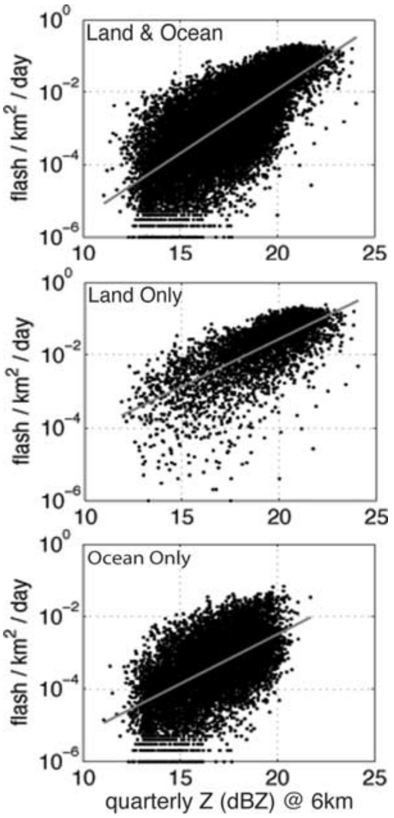

Figure 1. (top) Scatter-plot showing the average 6-km reflectivity in dB*Z* versus the average flash-rate on a log scale. Sampling is quarterly in time, 5 degrees in space. (middle) Same as top, but land only. (bottom) Same as top but ocean only. In each panel straight lines are regression lines between reflectivity and log of flash rate, with slope *a* and intercept *b*. Top, $a = 0.353$, $b = -8.98$. Middle, $a = 0.261$, $b = -6.77$. Bottom, $a = 0.272$, $b = -7.94$. Data cover the period December 1997 to November 2002.

represents the average flash rate and the average 6-km reflectivity at a fixed grid point in space and time. The plot shows that the averages of the flash rate and reflectivity are related, and, indeed, the correlation coefficient between the logarithm of the flash rate and the reflectivity in dBZ is 0.70, indicating fairly strong correlation. A similar analysis was performed using the 3B31 surface rain versus flash rate, resulting in a correlation coefficient of 0.44. *Petersen and Rutledge* [2001] also found a reduction in correlation of flash rate with surface rain versus upper-level reflectivity.

[6] Figure 1 (middle) shows the points from Figure 1 (top) that occurred over land, while Figure 1 (bottom) shows those points over ocean. The correlation coefficient of 6-km reflectivity versus flash rate is 0.71 over land, reduced to 0.58 over ocean. That there is still relatively large correlation over ocean agrees with *Toracinta et al.* [2002], who found that oceanic systems with lightning have reflectivity profiles that fall off less quickly with altitude than those without lightning. Note that the magnitudes of both flash rate and reflectivity in Figure 1 are much smaller over ocean than land, also in agreement with *Toracinta et al.* [2002]. The reduced correlation over the ocean could be related in part to the LIS detection threshold; the low oceanic flash rates may result in some undetected flashes [*Boccippio et al.*, 2002].

[7] Having confirmed the correlation between the averaged 6-km reflectivity and lighting, we next consider the spatial patterns of each. The EOFs for both variables were computed; the first EOFs are shown in Figure 2. The first EOF for lightning contains 61% of the variance, while the second EOF variance drops to 15%. The first EOF for reflectivity contains 40% of the total variance, while the second contains only 18%. Hence, the first EOFs for both lightning and reflectivity are dominant. These EOFs are similar to each other and to the lightning EOF of *Martin et al.* [2000], with most of the variability occurring over land. The principal component time series corresponding to the first EOFs both appear nearly sinusoidal with one-year period (not shown). The variability in the averaged lightning and reflectivity is, not surprisingly, dominated by seasonal changes.

[8] A more interesting time behavior is found by looking at the anomaly of lightning and reflectivity. The anomaly is found by subtracting the quarterly value averaged over all years from the quarterly value in a given year; this is performed for each spatial grid point and each quarter in the data sets. Figure 3 shows the first EOFs of the anomalies. Interestingly, the first EOF of the anomaly for reflectivity shows more variation over the ocean, while the lighting anomaly shows more variability over land. Also note that the first reflectivity anomaly EOF contains 29% of the total variance. The next EOF is much weaker, containing only 11% of the variance. In contrast, the first six lightning anomaly EOFs have variances of 20%, 17%, 15%, 10%, 8%, and 8%, respectively. Unlike the reflectivity anomaly, the lightning anomaly does not have a particularly dominant EOF.

[9] Figure 4 (top) shows the time series of the first and third lightning anomaly principal components. The time series is extended back to 1995 by including OTD data; the combined LIS/OTD product includes corrections for the different sensitivities of the two instruments. To reduce possible instrument effects, only LIS data were used to generate the EOFs; the combined LIS/OTD data were then

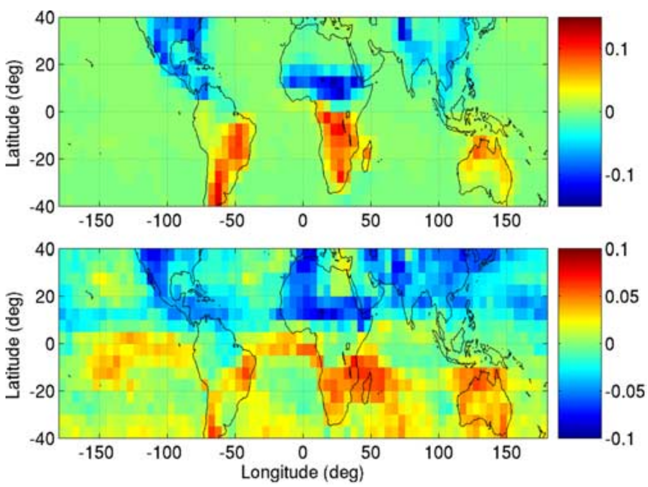

Figure 2. First EOF for lightning in flashes/km^2/day (top) and reflectivity in dBZ (bottom). Data cover the period December 1997 through May 2001.

projected on to the LIS EOFs. Also shown is the Southern Oscillation Index (SOI) [*Troup*, 1965] for the same period. The correlation coefficient with SOI is fairly high (0.72) for the first principal component and rather low (0.23) for the third principal component. The remaining four out of the first six principal components are essentially uncorrelated with SOI (correlation coefficient of 0.11 or less). Figure 4 (bottom) shows the SOI and reflectivity anomaly first principal component; they show similar behavior. The correlation coefficient in this case is 0.81, although the data record for reflectivity anomaly is shorter than for lightning anomaly. The correlations indicate that El Niño impacts both anomalies. The lack of a dominant lightning anomaly EOF and the lack of high correlation with SOI for five of the first six lightning anomaly principal components suggest that El Niño has a larger effect on the reflectivity anomaly. The role of El Niño in both anomalies is not unexpected, given the relatively short length of data and the very strong El Niño that occurred within the data record.

[10] Effects of El Niño on global lightning activity have been previously reported. *Watkins et al.* [2001] inferred changes in lightning activity via VLF sferics measurements. Increased lightning during El Niño was noted over the southeastern United States [*Goodman et al.*, 2000] and Indonesia [*Hamid et al.*, 2001], in agreement with our results in Figures 3 and 4. *Hamid et al.* [2001] noted a decrease in the number of convective storms over Indonesia during El Niño, while *Schumacher and Houze* [2003] found reduced stratiform rainfall fraction in that area. They also noted an increase in stratiform rainfall fraction in the central and eastern Pacific during El Niño. These findings by other investigators may be manifestations of the global effects of El Niño on lightning and reflectivity noted here.

4. Conclusions

[11] Satellite observations of average upper-level radar reflectivity and lightning over a 5-year period have shown high correlation. Both reflectivity and lightning flash rate tend to be much greater over land than ocean; however, they are well correlated even over the ocean. A weaker, but

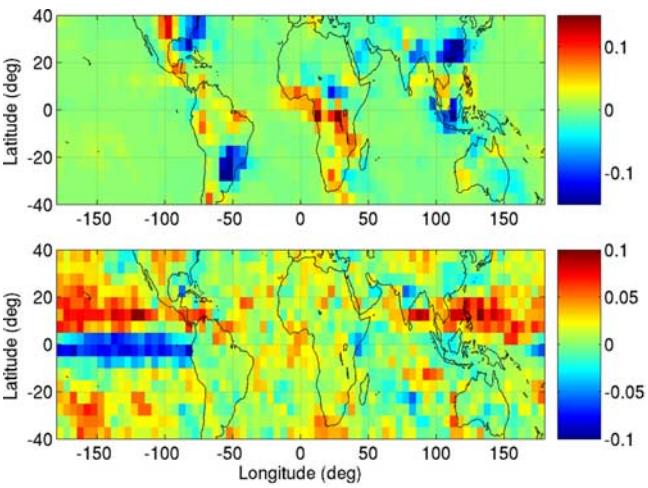

Figure 3. First EOF for anomalies of lightning in flashes/km^2/day (top) and reflectivity in dBZ (bottom). Data cover the period December 1997 through May 2001.

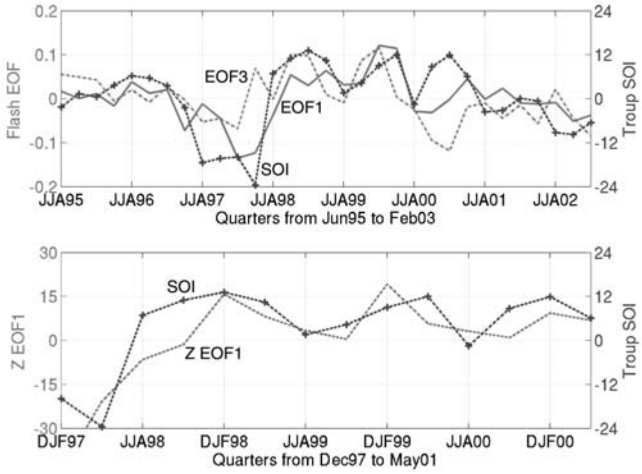

Figure 4. (top) First and third lightning anomaly principal components (based on LIS and OTD data), along with Southern Oscillation Index (SOI) for period June 1995 to February 2003. Lightning anomaly is solid line (EOF1) and dot-dashed line (EOF3), and SOI is dashed line with plus symbols. (bottom) First principal component of reflectivity anomaly and SOI (plus symbols) for December 1997 through May 2001.

moderate, correlation was also found between lightning flash rate and surface rainfall. First EOFs for averaged lightning and reflectivity are similar, showing most of the variability over land. In contrast, the EOFs of the lightning and reflectivity anomalies have different spatial patterns; however, both anomalies have principal component time series that are correlated with the SOI, indicating that El Niño impacts both. The reflectivity anomaly first principal component is well correlated with SOI, and its corresponding EOF can be considered dominant, since it contains substantially more variance than the second EOF (29% vs. 11%). The lack of a dominant lightning anomaly EOF and the lack of high correlation with SOI for five of the first six lightning anomaly principal components suggest that El Niño has a larger effect on the reflectivity anomaly.

[12] **Acknowledgments.** The research described in this paper was carried out at the Jet Propulsion Laboratory, California Institute of Technology, under contract with the National Aeronautics and Space Administration. Support from the NASA TRMM and Precipitation Science programs is gratefully acknowledged.

References

Boccippio, D. J., W. J. Koshak, and R. J. Blakeslee (2002), Performance assessment of the optical transient detector and lightning imaging sensor. Part I: Predicted diurnal variability, *J. Atmos. Oceanic Technol.*, *19*, 1318–1332.

Christian, H. J., et al. (2003), Global frequency and distribution of lightning as observed from space by the optical transient detector, *J. Geophys. Res.*, *108*(D1), 4005, doi:10.1029/2002JD002347.

Goodman, S. J., D. E. Buechler, K. Knupp, K. Driscoll, and E. W. McCaul (2000), The 1997–98 El Niño event and related wintertime lightning variations in the southeastern United States, *Geophys. Res. Lett.*, *27*, 541–544.

Hamid, E. Y., Z.-I. Kawasaki, and R. Mardiana (2001), Impact of the 1997–98 El Niño event on lightning activity over Indonesia, *Geophys. Res. Lett.*, *28*, 147–150.

MacGorman, D. R., and W. D. Rust (1998), *The Electrical Nature of Storms*, Oxford Univ. Press, New York.

Martin, R. V., D. J. Jacob, J. A. Logan, J. M. Ziemke, and R. Washington (2000), Detection of a lightning influence on tropical tropospheric ozone, *Geophys. Res. Lett.*, *27*, 1639–1642.

Petersen, W. A., and S. A. Rutledge (2001), Regional variability in tropical convection: Observations from TRMM, *J. Clim.*, *14*, 3566–3586.

Price, C., J. Penner, and M. Prather (1997), NO_x from lightning: 1. Global distribution based on lightning physics, *J. Geophys. Res.*, *102*, 5929–5941.

Schumacher, C., and R. A. Houze (2003), Stratiform rain in the tropics as seen by the TRMM precipitation radar, *J. Clim.*, *16*, 1739–1756.

Toracinta, E. R., D. J. Cecil, E. J. Zipser, and S. W. Nesbitt (2002), Radar, passive microwave, and lightning characteristics of precipitating systems in the tropics, *Mon. Weather Rev.*, *130*, 802–824.

Troup, A. J. (1965), Southern oscillation, *Q. J. R. Meteorol. Soc.*, *91*, 490–506.

Watkins, N. W., N. A. Bharmal, M. A. Clilverd, and A. J. Smith (2001), Comparison of VLF sferics intensities at Halley, Antarctica, with tropical lightning and temperature, *Radio Sci.*, *36*, 1053–1064.

Zipser, E. J., and K. R. Lutz (1994), The vertical profile of radar reflectivity of convective cells—A strong indicator of storm intensity and lightning probability?, *Mon. Weather Rev.*, *122*, 1751–1759.

S. L. Durden, Z. S. Haddad, and J. P. Meagher, Jet Propulsion Laboratory, California Institute of Technology, Pasadena, CA 91109, USA. (sdurden@jpl.nasa.gov)